Growth and morphology of 0.80 eV photoemitting indium nitride nanowires

M.C. Johnson, C.J. Lee, and E.D. Bourret-Courchesne*,

Lawrence Berkeley National Laboratory, Molecular Foundry, 1 Cyclotron Road, MS2R0200, Berkeley, CA 94720-8197, USA

S.L. Konsek, S. Aloni, W.Q. Han, and A. Zettl

Lawrence Berkeley National Laboratory, Molecular Foundry, 1 Cyclotron Road, MS66200, Berkeley, CA 94720-8197, USA

University of California, Department of Physics, Berkeley, CA 94720 USA

*Corresponding author: Edith Bourret-Courchesne, LBNL 1 Cyclotron Road, MS2R0200, Berkeley, CA 94720-8197, USA Phone (510)486-5553 Fax (510) 486-5530 email EDBourret@lbl.gov

Abstract

InN nanowires with high efficiency photoluminescence emission at 0.80 eV are reported for the first time. InN nanowires were synthesized via a vapor solid growth mechanism from high purity indium metal and ammonia. The products consist of only hexagonal wurtzite phase InN. Scanning electron microscopy showed wires with diameters of 50-100nm and having fairly smooth morphologies. High-resolution transmission electron microscopy revealed high quality, single crystal InN nanowires which grew in the <0001> direction.

The group-III nitrides have become an extremely important technological material over the past decade[1]. They are commonly used in optoelectronic devices, such as high brightness light-emitting diodes[2] (LEDs) and low wavelength laser diodes[3] (LDs), as well as high power/high frequency electronic devices[4,5]. Recently InN thin films grown by MOCVD and MBE were found to have a bandgap energy in the range of 0.7-0.9 eV[6-8], much lower than the value of ~1.9 eV found for InN films grown by sputtering[9]. This large decrease in the direct bandgap transition energy and the ability to form ternary (InGaN) and quaternary (AlInGaN) alloys increases the versatility of group-III nitride optoelectronic devices, ranging from the near IR to the UV. Additionally, InN has some promising transport and electronic properties. It has the smallest effective electron mass of all the group-III nitrides which leads to high mobility and high saturation velocity[10] and a large drift velocity at room temperature[4,5,11]. As a result of these unique properties, there has been a large increase in interest in InN for potential use in optoelectronic devices, such as LDs and high efficiency solar cells, as well as high frequency/high power electronic devices.

Unfortunately, high quality InN is very difficult to synthesize. It has a very low decomposition temperature and requires a large overpressure of N. There are only a few reports on thin film deposition of InN[12-17] and on the one- dimensional synthesis of InN nanostructures. Vapor-solid growth of InN nanowires using a mixture of In metal/In_2O_3 powder and ammonia has been reported[18]. Other InN nanostructure synthesis methods use a solvo-thermal method[19], halide chemical vapor deposition (CVD)[20], CVD using single-source precursors $N_3In[(CH_2)_3NMe_2]_2$[21], and ammonolysis of indium oxide[22]. There are also reports on the synthesis of more advanced structures such as InN/InP core/sheath nanowires[23] and InN/GaN nanoheterojunctions[24] as well as the catalytic selective area growth on gold

patterned Si(100) substrates[25]. These wires obtained by this catalytic growth technique exhibit a broad photoluminescence (PL) at 1.85 eV. To our knowledge, a method for synthesizing one-dimensional photo emitting structures in the range of 0.7-0.9 eV has not been reported.

In this letter, we report for the first time the synthesis of single crystal, 0.80 eV photo-emitting InN nanowires using In metal and ammonia. The InN nanostructures are formed using a vapor solid growth mechanism deposited on both the quartz surface and the In source metal surface.

The growth of InN nanowires was performed in a high temperature tube furnace with a quartz tube. High purity In metal (99.999%) was placed in a quartz boat in contact with a thermocouple to assure accurate growth temperature measurement. High purity ammonia (5N) flowed at 200 sccm for 1 hour while the temperature was being ramped to a final growth temperature of 700°C. The furnace was held constant at this temperature while ammonia was flowed over the quartz boat at 600 sccm for 2 hours. The samples were rapidly cooled down to room temperature under ammonia flow before being purged with N_2. The samples were collected from both the surface of the In metal and from the surface of the quartz boat up to 2 cm downstream of the In source metal. Structural and compositional characterization were performed using powder x-ray diffraction (XRD) (Bruker D-8 GADDS) with a CoK_α x-ray source, scanning electron microscopy (SEM) using a FEI Sirion 75 microscope equipped with an electron energy-dispersive spectrometer (EDS), and high resolution transmission electron microscopy (TEM) using a JEOL 2011 capable of selective area electron diffraction (SAD) and nanobeam electron diffraction (NBD). Optical characterization was performed using room-temperature photoluminescence. The

photoluminescence signals were generated in the backscattering geometry by excitation with the 515 nm line of an argon laser. The emission signals were dispersed by a 1 m double-grating monochromator and detected by a LN2 cooled Ge detector.

Figure 1a shows a typical SEM image of InN nanowires taken from the surface of the quartz boat. Typical nanowire diameters were in the range of 50-100 nm with typical lengths of several microns. The surface morphology of the nanowire as shown in the inset of Figure 1a appears smoother than the morphologies of wires obtained from other growth strategies for InN[18,23]. Figure 1b shows the corresponding EDS spectrum for an individual nanowire indicating that the nanowires consist of In and N in an atomic ratio of approximately 1:1. These results were reproducible over many growth runs which show that this technique is capable of synthesizing compositionally uniform InN nanowires.

Figure 2 shows the XRD pattern for InN nanowires. All the diffraction peaks in the spectrum are indexed to be hexagonal wurtzite phase. The lattice parameters were calculated to be a = 3.52 Å and c = 5.71 Å which is in good agreement with the reported values of bulk InN. The strong intensities of the InN diffracted peaks and the absence of any indium oxide peaks indicate that the InN nanowires are of high purity and the sample consists of only wurtzite phase material.

HRTEM study unravels more detailed structural and morphological information. Figure 3a and 3b shows a typical InN nanowire. Although the diameter fluctuates by about 30% along the nanowire, we find that the wire is monolithic single crystalline material growing in the <0001> direction. Figure 3c displays the high quality of the nanowire showing the (002) planes perpendicular to the wire axis with an inter-lattice spacing of 0.286 nm. Figure 3d shows the NBD patterns where the unit cell constants are measured to be

a = 3.50 Å and c = 5.70 Å which are in good agreement with the measurements from XRD studies.

These wires grew directly on the quartz boat with no intentional catalysts present indicating that the growth mechanism was governed by a vapor-solid process. Further optimization of the growth parameters should allow growth of smoother and thinner wires.

Figure 4 shows the room-temperature photoluminescence spectrum for as-grown InN nanowires. The photoluminescence peak emission is located at 0.80 eV which is consistent with literature results reporting a bandgap energy emission in the range of 0.70-0.90 eV[6-8]. More importantly, the emission was extremely intense relative to the amount of material produced and the low incident laser power used (9mW) although a quantum efficiency cannot be determined from these measurements at this time. The PL emission from these nanowires was compared to high quality material thin films grown using Metalorganic Chemical Vapor Deposition (MOCVD)[12] as shown in Figure 4. It is clear that these single crystalline nanowires have a very similar emission spectrum but with a narrower full width at half maximum (FWHM) indicating a higher quality material. Additionally, the peak emission is red-shifted by 30 meV which indicates a lower bandgap energy than the thin film. These PL results show the possibility of determining fundamental properties of InN from nanosize material eliminating many of the dislocations and impurities inherent to thin film materials. More detailed studies of the optical and transport properties of these InN nanowires are being investigated.

In conclusion, we have developed a simple and reproducible method by which we can synthesize InN nanowires with a vapor solid growth process using In metal and ammonia as the reactant species. SEM and EDS show that the wires range between 50-100nm in

diameter with lengths up to several microns and consist of high purity InN. TEM results show that the wires are single crystal growing in the <001>. The photoluminescence emission is highly efficient with a peak emission energy at 0.80 eV. To our knowledge, this is the first time that PL emission at 0.80 eV is reported for InN nanowires. The growth mechanism is still being investigated but this simple technique appears promising for developing high efficiency InN-based nanosize optoelectronic devices.

Acknowledgement

This work was supported by the Director, Office of Science, Office of Basic Energy Sciences, Division of Materials Science and Engineering, of the U.S. Department of Energy under Contract No. DE-AC03-76SF00098.

References

1. S. Nakamura, S. Pearton, and G. Fasol, *The Blue Laser Diode, The Complete Story*, Springer-Verlag, Germany, 2000.
2. Y.C. Shen, J.J. Wierer, M.R. Krames, M.J. Ludowise, M.S. Misra, F. Ahmed, A.Y. Kim, G.O. Mueller, J.C. Bhat, S.A. Stockman, and P.S. Martin, Applied Physics Letters **82**(2003)2221.
3. S. Nagahama, T. Yanamoto, M. Sano, and T. Mukai,, Appl. Phys. Lett. **79**(2001)1948.
4. S.K. O'Leary, B.E. Foutz, M.S. Shur, U.V. Bhapkar, and L.F. Eastman, J. Appl. Phys. **83**(1997)826.
5. E. Bellotti, B.K. Doshi, K.F. Brennan, J.D. Albrecht, and P.P. Ruden, J. Appl. Phys. **85**(1999)916.
6. J. Wu, W. Walukiewicz, K.M. Yu, J.W. Ager III, E.E. Haller, H. Lu, W.J. Schaff, Y. Saito, and Y. Nanishi, Appl. Phys. Letts. **80**(2002)3967.
7. T. Inushima, V.V. Mamutin, V.A. Vekshinb, S.V. Ivanov, T. Sakon, M. Motokawa, and S. Ohoya, J. Crystal Growth **227-228**(2001)481.
8. V. Yu. Davydov, A.A. Klochikhin, R.P. Seisyan, V.V. Emtsev, S.V. Ivanov, F. Bechstedt, J. Furthmuller, H. Harima, A.V. Mudryi, J. Aderhold, O. Semchinova, and J. Graul, Phys. Status Solidi B **229**(2002)R1.
9. S. Inoue, T. Namazu, T. Suda, and K. Koterazawa, Vacuum **74**(2004)443.
10. S.N. Mohammad and H. Morkoc, Prog. Quantum Electron. **20**(1996)361.
11. B.E. Foutz, S.K. O'Leary, and M.S. Shur, L.F. Eastman, J. Appl. Phys. **85**(1999)7727.
12. M.C. Johnson, S.L. Konsek, A. Zettl, and E.D. Bourret-Courchesne, J. Crystal Growth (accepted June 2004).

13. R.S.Q. Fareed, R. Jain, R. Gaska, M.S. Shur, J. Wu, W. Walukiewicz, and M.A. Khan, Appl. Phys. Letts. **84**(2004)1892.

14. F.H. Yang, J.S. Hwang, K.H. Chen, Y.J. Yang, T.H. Lee, L.G. Hwa, and L.C. Chen, Thin Solid Films **405**(2002)194.

15. A. Yamamoto, M. Adachi, and A. Hashimoto, J. Cryst. Growth **230**(2001)351.

16. A.G. Bhuiyan, A. Yamamoto, A. Hashimoto, and Y. Ito, J. Cryst. Growth **236**(2002)59.

17. T. Yodo, H, Yona, H. Ando, D. Nosei, and Y. Harada, Appl. Phys. Lett. **80**(2002)968.

18. J. Zhang, L. Zhang, X. Peng, and X. Wang, J. Mater. Chem. **12**(2002)802.

19. Y.J. Bai, Z.G. Liu, X.G. Xu, D.L. Cui, X.P. Hao, X. Feng, and Q.L. Wang, J. Crystal Growth **241**(2002)189.

20. N. Takahashi, A. Niwa, T. Takahashi, T. Nakamura, M. Yoshioka, and Y. Monose, J. Mater. Chem. **12**(2002)1573.

21. H. Parala, A. Devi, F. Hipler, E. Maile, A. Birkner, H.W. Becker, and R.A. Fischer, J. Crystal Growth **231**(2001)68.

22. B. Schwenzer, L. Loeffler, R. Seshadri, S. Keller, F.F. Lange, S.P. DenBaars, and U.K. Mishra, J. Mater. Chem. **14**(2004)637.

23. L.W. Yin, Y. Brando, Y.C. Zhu, D. Golberg, and M.S. Li, Appl. Phys. Letts. **84**(2004)1546.

24. Z.H. Lan, C.H. Liang, C.W. Hsu, C.T. Wu, H.M. Lin, S. Dhara, K.H. Chen, L.C. Chen, and C.C. Chen, Adv. Funct. Mater. **14**(2004)233.

25. C.H. Liang, L.C. Chen, J.S. Hwang, K.H. Chen, Y.T. Hung, and Y.F. Chen, Appl. Phys. Letts. **81**(2002)22.

Figure Captions

Figure 1 – (a) Typical SEM image of InN nanowires. The diameters of the wires range from 50-100 nm with some thick InN ribbons. The inset is a typical high magnification image of a single InN nanowire. (b) EDS of a single InN nanowire show that the resulting wires are pure InN.

Figure 2 – XRD spectrum for InN nanowires grown at 700°C using indium metal and ammonia. InN nanowires consist of only the hexagonal wurtzite phase with the corresponding indices marked above the respective diffraction peak.

Figure 3 – (a) Typical TEM image of an individual InN nanowire. (b) High magnification TEM image of InN nanowire. Nanowires have a diameter that fluctuates between 50-100nm. (c) High resolution TEM image of InN nanowire showing lattice spacing of the (002) planes to be 0.286 nm. (d) Nanobeam electron diffraction of InN nanowire.

Figure 4 – Room-temperature PL of bulk InN nanowires compared to MOCVD grown InN thin film. The peak emission energy of the nanowires is 0.80 eV.

Figure 1

Figure 1a

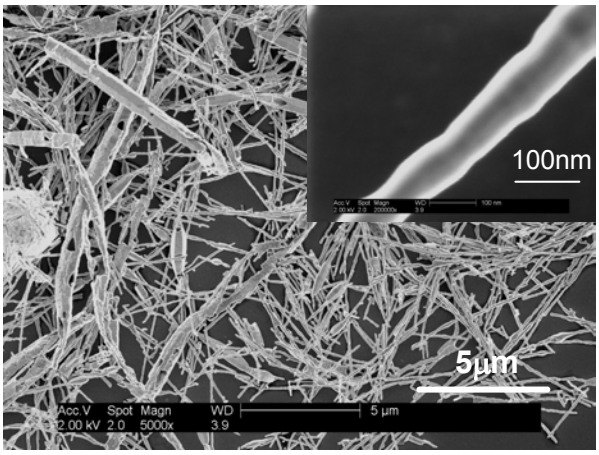

Figure 1b

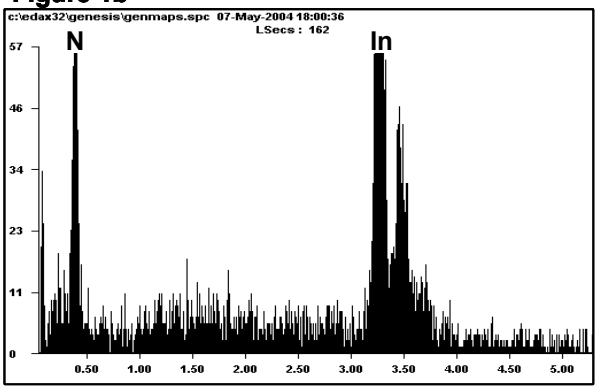

Figure 2

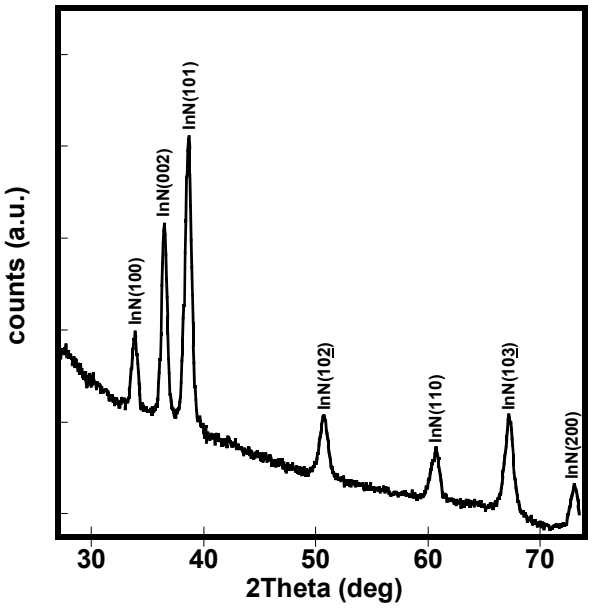
counts (a.u.)
InN(100)
InN(002)
InN(101)
InN(10$\bar{2}$)
InN(110)
InN(10$\bar{3}$)
InN(200)
30
40
50
60
70
2Theta (deg)

Figure 3

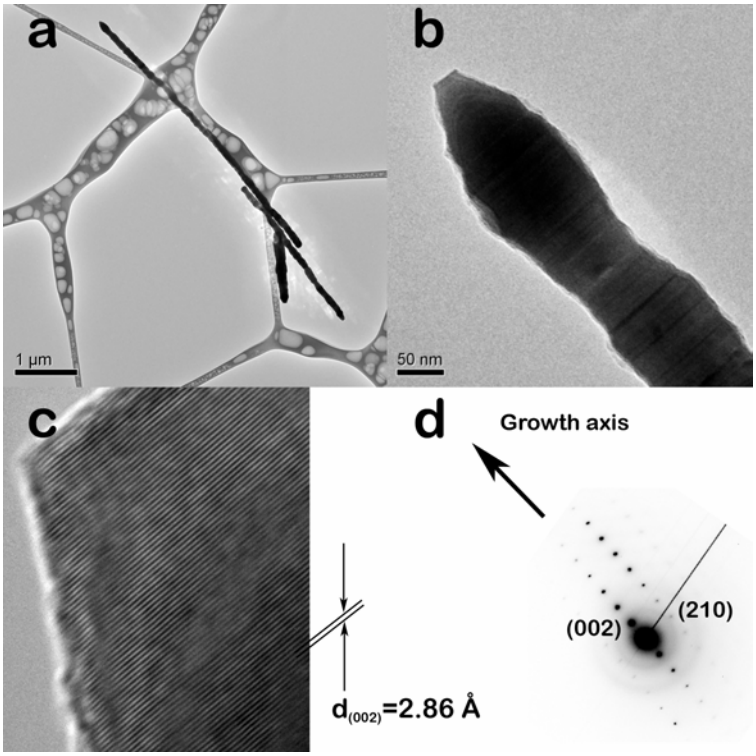

Figure 4

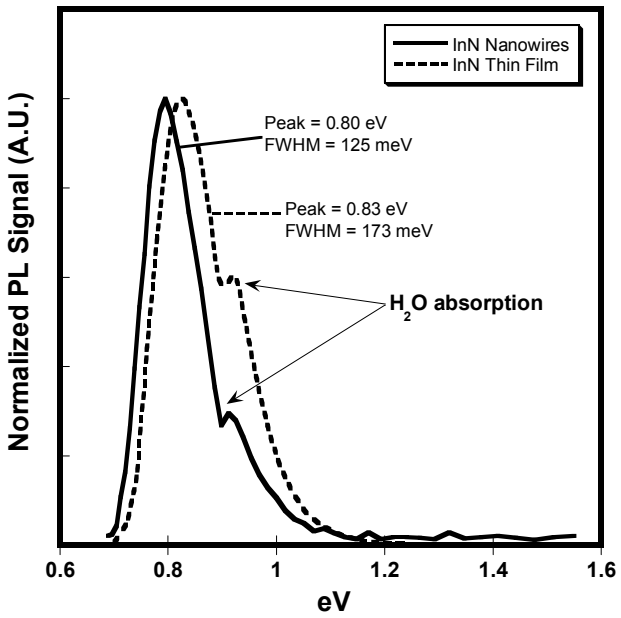
InN Nanowires
InN Thin Film
Peak = 0.80 eV
FWHM = 125 meV
Peak = 0.83 eV
FWHM = 173 meV
H2O absorption
Normalized PL Signal (A.U.)
0.6
0.8
1
1.2
1.4
1.6
eV